CHEMISTRY

Microscale mechanochemical characterization of drying oil films by in situ correlative Brillouin and Raman spectroscopy

Martina Alunni Cardinali[1], Laura Cartechini[2], Marco Paolantoni[1], Costanza Miliani[3], Daniele Fioretto[4,5], Luciano Pensabene Buemi[6], Lucia Comez[5]*, Francesca Rosi[2]*

Correlative Brillouin and Raman microspectroscopy (BRaMS) is applied for the in situ monitoring of the chemical and physical changes of linseed oil during polymerization. The viscoelastic properties of the drying oil throughout the phase transition were determined by Brillouin light scattering (BLS) and joined to the Raman spectroscopic information about the chemical process responsible for the oil hardening. A comparative study was then performed on an oil mock-up containing ZnO, one of the most common white pigments used in cultural heritage. The intriguing outcomes open new research perspectives for a deeper comprehension of the processes leading to the conversion of a fluid binder into a dry adhering film. The description of both chemical and structural properties of the polymeric network and their evolution are the basis for a better understanding of oil painting degradation. Last, as a feasibility test, BRaMS was applied to study a precious microfragment from J. Pollock's masterpiece *Alchemy*.

INTRODUCTION

Since antiquity, drying oils (also called siccative oils) have been used as painting media, thanks to their ability to dry through polymerization, forming a solid film with good mechanical and optical properties, keeping the pigment particles firmly bound and adhering to the support. The introduction of siccative oil as a binder in art marked a turning point that allows artists to obtain enhanced optical effects, model the painted surface, and create a sense of depth and relief, which are not possible with the tempera-based painting techniques (*1*). Today, they are still in use not only in art but also as components in modern coatings such as alkyd paints or polyester resins. The hardening of drying oils is a chemical transformation, which occurs via an autoxidative process followed by polymerization (*2*, *3*). Despite the long history of research studies on the drying mechanism, which dates to the early '20s (*4*, *5*), it is still a vivid research focus (*6*), especially in relation to the common degradation phenomena of oil paints and consequent conservation issues (*7*). The hardening process conditions, the chemical nature, and the structural properties of the final polymeric network strongly influence the way the film ages and degrades thereafter (*4*). Stiffening and embrittlement of oil paints, wrinkling, cracking, flaking, and delamination due to the rupture in the polymeric network, together with the increased sensitivity to water and solvents (which inhibits cleaning interventions), are all long-standing issues for conservators (*8*–*10*). The alteration of oil paints is a complex and synergic process depending on many interplaying factors, including paint composition and thickness, environment, and solvent exposure, among others (*11*). Film degradation is the result of both chemical and mechanical changes that are intimately connected, requiring complementary and interrelated investigations to have a full comprehension of the process at the molecular level. So far, a great amount of research has focused on the separate chemical and mechanical characterization of paint films through independent approaches, often because of the impossibility of using the same sample with techniques that require different sample preparation procedures (*10*). Furthermore, there is a lack of analytical methodologies able to simultaneously monitor in situ and in real time these changes during the formation of the oil film and its progressive alterations.

With the present paper, we propose combined measurements of Brillouin light scattering (BLS) and Raman in a microspectroscopic setup (BRaMS) as a new approach potentially able to fill this gap (*12*). BLS deals with the inelastic scattering of light from thermally activated acoustic waves in the gigahertz range (order of tens of gigahertz), providing information about the elastic and viscoelastic properties of materials probed in a unique time/frequency range, which are inaccessible by traditional tensile testing (fixed stress-strain conditions) (*13*–*16*). Furthermore, BLS probes mechanical properties without any external perturbations of the system, as is usually the case in dynamic mechanical analysis, where it is necessary to apply oscillatory loading conditions via disposable plates, cantilevers, or film tension grips (*17*, *18*). BLS has established itself as a powerful analytical tool in condensed matter physics and material science for years. Improvements in instrumentation and the conception of new experimental setups have fostered a growing interest for application of the technique in new fields such as biology, biomedicine, and bioengineering (*16*, *19*–*22*).

In a complementary way, Raman spectroscopy is based on the light scattered by optical phonons or intramolecular vibrations at super terahertz frequencies. It is widely applied to in situ molecular characterization of substrates and matrices, used in several fields from physics to chemistry and biomedicine, and has demonstrated to be a powerful analytical tool also in heritage science (*23*, *24*). In this study, we benefited from a recently proposed instrumental

[1]Department of Chemistry, Biology and Biotechnology, University of Perugia, Via Elce di Sotto, 6 06123 Perugia, Italy. [2]Institute of Chemical Sciences and Technologies-SCITEC, National Research Council-CNR, Via Elce di Sotto, Perugia I-06123, Italy. [3]Institute of Heritage Science-ISPC, National Research Council-CNR, Via Cardinale Guglielmo Sanfelice 8, 80134 Napoli (NA), Italy. [4]Department of Physics and Geology, University of Perugia, Via Pascoli, Perugia I-06123, Italy. [5]Istituto Officina dei Materiali-IOM, National Research Council-CNR, Via Pascoli, Perugia I-06123, Italy. [6]Peggy Guggenheim Collection, Dorsoduro, 701-704, 30123 Venezia, Italy.
*Corresponding author. Email: francesca.rosi@cnr.it (F.R.); comez@iom.cnr.it (L. Co.)

configuration where BLS and Raman devices have been coupled in a microspectroscopic setup, enabling the simultaneous noninvasive chemical and mechanical characterization of samples and mapping at a micrometric spatial resolution (*12*). This combined approach has proven to be very effective in the phenotyping of biological systems, which are characterized by an intrinsic complexity and heterogeneity (*16*, *25*–*30*).

Inspired by these previous remarkable works, here, BRaMS has been exploited to study painting components, which represent another class of likewise complex and variegated materials characterized by issues still far to be solved. This study aims to assess the potential of BRaMS for the investigation of oil paint films, understanding molecular and structural changes that occur during polymerization and curing, and, in perspective, to define paint stability. To validate the feasibility of the approach, the first BRaMS spectra were recorded on a real microfragment taken from the iconic painting *Alchemy*, a masterpiece of American abstract expressionism.

RESULTS

BLS-Raman microspectroscopy of drying oil

The experimental setup is reproduced in Fig. 1A. Figure 1B shows the first Brillouin and Raman spectra simultaneously acquired on the same spot of a thin layer of linseed oil (a siccative oil) at different times of polymerization. The drying of the oil was monitored for 23 consecutive days, recording BLS-Raman spectra in different points to reduce the intrasample variability (at least three per day). The measured Brillouin peak is linked to (i) the real part of the longitudinal modulus, M', and (ii) the acoustic absorption, α, of the elastic waves arising from spontaneously collective density fluctuations, propagating in all directions within the sample. M' and α can be directly derived from the position and full width at half maximum of the peak (details of the calculations are reported in the Supplementary Materials). In this study, the advantage of deriving such viscoelastic properties at gigahertz frequencies comes from the opportunity of monitoring in real time and in situ the phase transition of drying oil, in which the molecular events triggering the polymerization take place on the time scale of hundreds of picoseconds (*31*).

From a chemical point of view, Raman spectra are sensitive to molecular changes of the polyunsaturated oil triglycerides, which, during polymerization, undergo conjugation and cis-to-trans isomerization of the unsaturated bonds, followed by their loss (*32*). During the drying process, the BLS peak of the oil discloses a considerable spectral change in frequency (Figs. 1B and 2, A and B). By close inspection of the peak shift of the BLS signal in the considered period (Fig. 2A, red filled circles), there is evidence of an abrupt frequency increase at about 8 days, beyond which it reaches a plateau with a maximum value of 13.4 GHz. More quantitatively, the sudden growth in the elastic modulus values (Fig. 2B, red filled circles), accompanied by the decrease in acoustic absorption (Fig. 2B, inset, green symbols), testifies a liquid-to-solid phase transition of the film, consistent with an elastic deformation of the linseed oil under stress drying from 2.5 to 5.5 GPa (percentage variation of M' more than 100%). In coincidence with the steep shift observed for the BLS peak (Fig. 2A), the Raman study reveals a sharp decrease and then disappearance of the $\nu(\text{=C—H})_{cis}$ band at 3014 cm^{-1} (Fig. 2A, black filled circle), indicative of the consumption of the nonconjugated cis-unsaturated bonds during the autoxidation process (*33*, *34*). At the same time (8 days), the nonconjugated $\nu(\text{C=C})_{cis}$ stretching band at 1660 cm^{-1} (Fig. 2C) rapidly broadens and downshifts, indicating both the formation of conjugated double bonds and cis/trans isomerization (*35*, *36*). The successive intensity decrease (consumption) of the ν(C=C) bands around 1660 cm^{-1} (after 9 days; Fig. 2C) is symptomatic of the progress of the cross-linking reaction and corresponds to the plateau regime for the BLS peak position.

In-depth probing of the mechanochemical properties of drying oil

The optical configuration of the experimental setup enables us also to perform in-depth Z-profiles (as well as surface XY mapping), probing the progress of polymerization at different depths inside

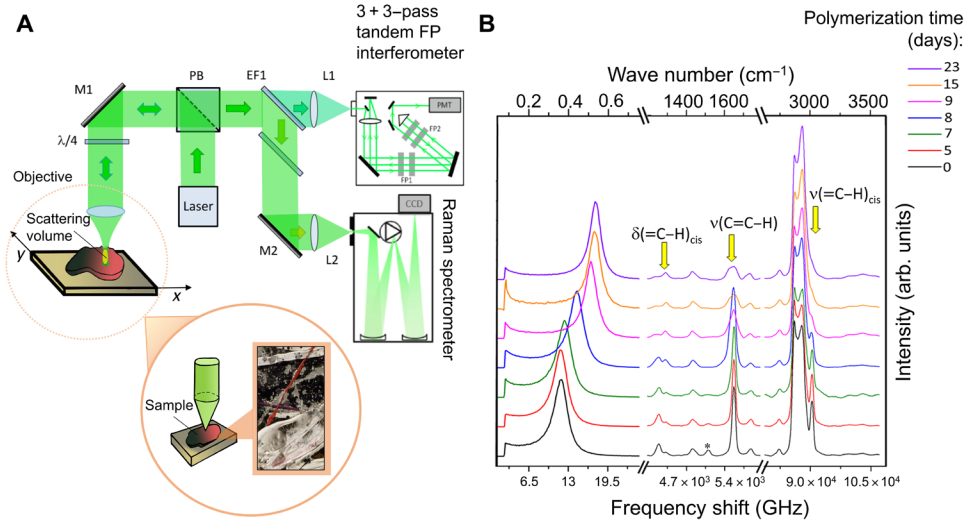

Fig. 1. BRaMS setup and spectra acquired during the oil drying. (**A**) Schematic representation of the micro-setup and figurative image of a white oil paint from an artwork (*Alchemy* by J. Pollock); (**B**) in situ multimodal Brillouin and Raman microspectroscopy (λ_{exc} = 532 nm) following the polymerization of linseed oil. Asterisk marks carotenoids already present in the oil formulation as antioxidants (*33*). PB, polarizing beamsplitter; PMT, photomultiplier tube; CCD, charge-coupled device; FP, Fabry Pérot; EF, edge filter; M, mirror; L, lens.

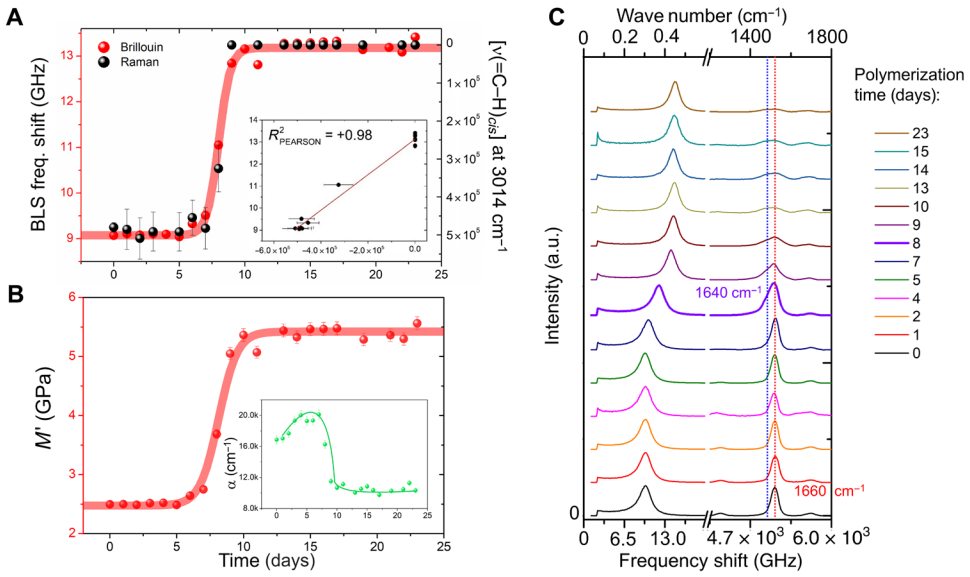

Fig. 2. Chemical and mechanical modifications during oil drying. (**A**) Correlative Brillouin and Raman investigation of oil polymerization: BLS frequency shift (red filled circles) and intensity of the [ν(=C–H)$_{cis}$] at 3014 cm^{-1} (black filled circles); (**B**) longitudinal elastic modulus, *M*′ (red filled circle), and acoustic absorption, α, (inset, green filled circles) variation; (**C**) spectral variation of the BLS peak and the [ν(C=C)] Raman band shifting from 1660 to 1640 cm^{-1}. Red and green lines in (A) and (B) are drawn only to guide the viewer's eye. a.u., arbitrary units.

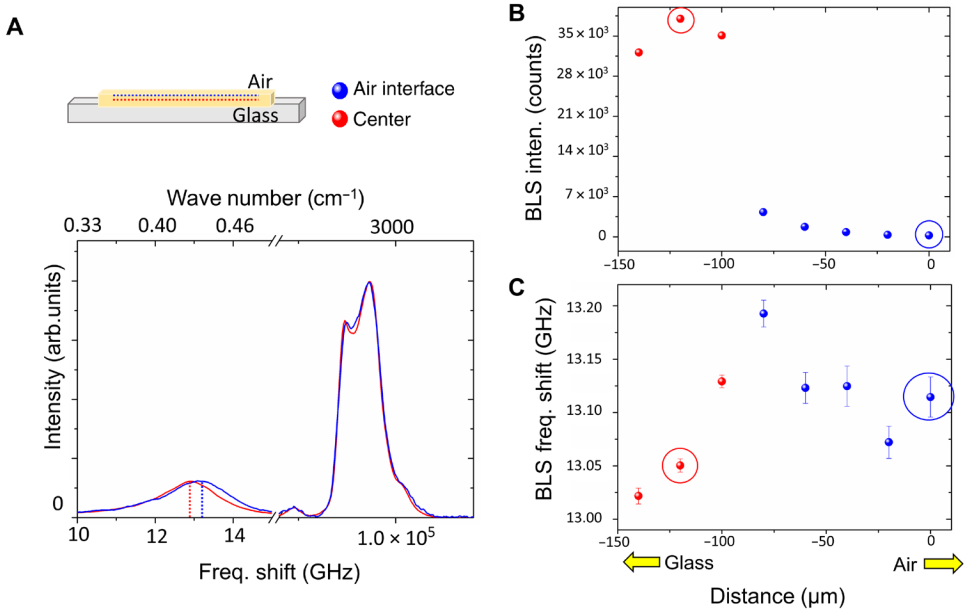

Fig. 3. In-depth probing of the progress of polymerization. (**A**) In situ multimodal BLS and Raman spectra at the air-sample interface (blue line) and 120 μm below the surface (red line) (normalized spectra); (**B**) variation of the BLS peak intensity and (**C**) BLS peak position at different depths. The circled points refer to the spectra selected for comparison.

the sample with an axial resolution of a few micrometers. Figure 3A reports the BRaMS measurements collected at the surface and inside the oil layer [at the air-sample interface (blue) and at about 100 μm inside the layer (red)] after 9 days of drying. Moving from the inside toward the surface, a decrease in the BLS signal intensity and a slight increase in the frequency shift can be observed (Fig. 3, B and C), suggesting that the oil surface layer directly in contact with the atmospheric oxygen (corresponding to the minimum of BLS intensity) is stiffer than the inner layers and thus is in an advanced polymerization state.

These local modulations in the frequency shift (from 13.05 to 13.12 GHz) correspond to a variation of about 1% in the longitudinal elastic modulus through the oil film (Fig. 3C). These results testify how the high-performance instrumentation used here, together with the BRaMS multimodal approach, is able to probe in situ

different degrees of polymerization of artists' paints, leveraging in-depth monitoring without sample manipulation.

BRaMS of a ZnO-oil paint mock-up

A fundamental role in the drying mechanism of siccative oil is played by the presence of pigments that influence both the cross-linking and photooxidation, thus affecting the final chemical and mechanical film stability (*11*). To figure out these issues, we performed BLS measurements on a sample simulating an oil paint with zinc oxide (Fig. 4A), one of the most common white pigments since the late 18th century (*37*). Figure 4 underlines the power of BLS to probe the phase transition also in these nontransparent samples, by monitoring the frequency shift of the peak during polymerization.

It is worth noting that although vibrational spectroscopy is already known as a powerful method for the identification of pigment in cultural heritage applications (*23*), the use of BLS for investigating the oil properties in the presence of dispersed solid particles of pigment was not so obvious, at least until the advent of high-contrast BLS microspectroscopy (*12*). Several considerations can be made from these measurements. The polymerization process was found to be faster in the presence of the ZnO pigment, as shown by the abrupt change of the longitudinal modulus just 2 days after the preparation (Fig. 4, B and C), in agreement with previous studies (*38*, *39*). A complementary probing of the chemical transformation of the oil was conducted by means of both the correlative Raman analysis (Fig. 4D, top) and transmission Fourier transform infrared (FT-IR) measurements (*40*) (Fig. 4D, bottom), using deposition of the same paint spread on a KBr pellet. The phase transition is clearly underlined by the broadening of the nonconjugated $\nu(C{=}C)_{cis}$ Raman band at 1660 cm^{-1}, as already seen for the pure oil sample. Furthermore, the FT-IR study was able to correlate the appearance of a broad band at about 1590 cm^{-1} to the sharp shift of the BLS peak, in correspondence with the liquid-to-solid transition. The attribution of this band is still controversial; it has been assigned to ZnO passivated by carboxylic acids (*41*) and to Zn-ionomer structures (*42*). Although a conclusive answer cannot be provided, with these data, we demonstrated that the appearance of this band is temporally connected with the liquid-to-solid phase transition of oil during polymerization. Moreover, the direct comparison of the BLS frequency shift of pure and ZnO-oil samples reported in Fig. 4B discloses that the addition of the pigment leads to a greater hardening (13.7 GHz) with respect to pure oil (13.4 GHz). Last, for the pigmented sample, further small variations in the position of the peak are visible at long time scales, suggesting that the system is still changing in terms of mechanical properties. A thorough interpretation of these findings needs further monitoring tests on both naturally and artificially aged samples and in the presence of different pigments, and it will be the object of a following publication.

BRaMS of a microfragment from *Alchemy* (1947)

To validate the feasibility of the proposed multimodal approach facing the complexity of actual painting materials, BRaMS experiments were carried out on a precious microfragment sampled from a white paint of J. Pollock's masterpiece *Alchemy*, 1947 (Fig. 5). The white paint is a mixture of ZnO and TiO_2 (anatase polymorph) in an oil medium (*43*). The extraordinarily intense Raman scattering of anatase dominates the Raman spectrum with bands at 640, 517, and 390 cm^{-1} (*43*), covering all other possible signals (*44*). The BLS profiles show the Brillouin peak centered at about 16 GHz, which is reproducible in different points of the sample, underlying a relatively homogeneous texture. The obtained BLS frequency position is higher with respect to the ZnO-oil model paint (16 and 14 GHz, respectively), meaning a harder oil film, compatible with a long curing/aging time of the paint while not excluding a consolidating effect due to the inorganic pigment mixture (*45*). This final example demonstrates the strength of the proposed approach to probing both the composition and mechanical properties even of complex and heterogeneous matrices, such as those of precious real artworks.

DISCUSSION

The aim of this first experiment was primarily to assess the value of BLS for investigating the viscoelastic properties of oil paintings at a time scale of hundreds of picoseconds, which are hardly reachable

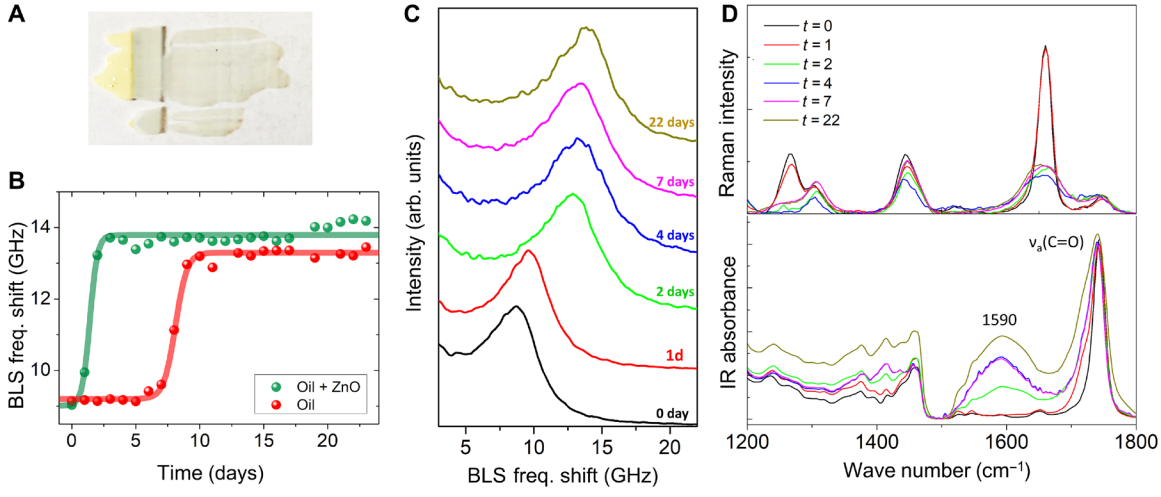

Fig. 4. BRaMS of ZnO-oil paint drying. (**A**) Image of the ZnO–linseed oil paint applied on a glass slide; (**B**) BLS frequency shift observed for the pure linseed oil sample (red line) and the ZnO–linseed oil paint sample (green line); (**C**) BLS microspectroscopy following the polymerization of a ZnO–linseed oil paint; (**D**) Raman spectra (top) and FT-IR spectra recorded in transmission mode (bottom) from a ZnO–linseed oil paint sample on a KBr pellet during polymerization. *t* = polymerization time (days).

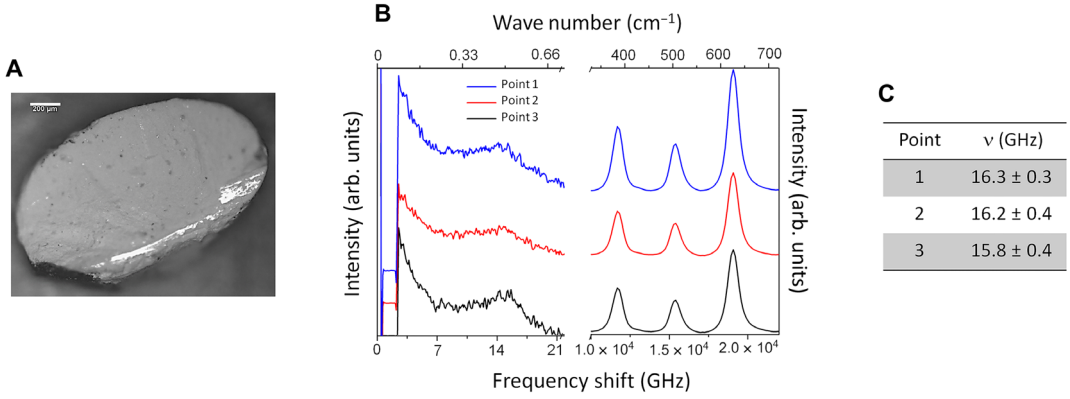

Fig. 5. Multimodal BRaMS of a microfragment sampled from J. Pollock's masterpiece *Alchemy*. (**A**) Optical image of the microfragment of the oil white paint sampled from *Alchemy*; (**B**) Brillouin and Raman spectra acquired on three different points of the sample; (**C**) Damped harmonic oscillator (DHO) fitting (eq. S1) results for the Brillouin shift are reported in the table.

by other methods. We demonstrated here that the multimodal BRaMS approach is effective for combined investigations of the viscoelastic and chemical properties of oil paint mock-up samples at high lateral and in-depth resolution.

In the field of heritage science, this new methodology opens interesting research perspectives for solving crucial issues in the conservation of oil paints. In the near future, the possibility of simultaneous investigations of the chemical and mechanical properties of a paint film, here monitored during drying of the pure oil and the ZnO-oil paint, could be exploited to study the following:

1) the relationship among the cross-linking mechanism and the elastic properties defined at both the molecular level and the macroscale (*18*);

2) the chemical and mechanical changes due to aging (*2*);

3) the effect of external environmental factors on the oil paint drying and the final mechanical-chemical stability (*18*, *46*);

4) the effect of the paint composition (different pigments and different oils including both traditional and modern ones) (*47*);

5) the effect of the oil-pigment interaction (i.e., the effect of the soap formation/migration and mechanical destabilization) (*39*, *48*, *49*);

6) the chemical and mechanical changes of oil paint during cleaning interventions (*50*, *51*).

Furthermore, the used setup has also proven effective to investigate samples from actual paintings, represented here by a microfragment taken from the *Alchemy*, the first highly experimental "drip" work of Pollock and a masterpiece of American abstract expressionism. This result entails the possibility of directly correlating the laboratory experimentation with issues inherent to a specific condition of an artwork.

Last, this proof-of-concept methodology with the present benchtop configuration would be a standpoint for investigations in the laboratory also on transportable precious objects. However, considering the enormous interest in designing combined portable devices for clinical and diagnostic applications, we cannot exclude that a further upgrade of the instrumentation will lead to new portable tools available in a short time.

MATERIALS AND METHODS

Experimental design

The experiments were carried out on dedicated model samples prepared ad hoc for following the drying process that was monitored through a multimodal approach based on the use of BRaMS and FT-IR spectroscopies.

Samples

Model sample preparation

Pure liquid linseed oil was supplied by Zecchi, and ZnO–linseed oil paint sample was prepared by mixing the same linseed oil with ZnO (Sigma-Aldrich) at a ratio of 1:1 in weight. For BRaMS experiments, the samples were applied as a thin layer on a glass slide, and different pressures were applied to obtain a gradient of thickness to evaluate the repercussions on the BLS spectral features. Then, since the BLS spectra quality was unaffected by the sample thickness, the measurements were performed in the thinner portion at each control to have comparable thicknesses with the corresponding samples spread in the KBr pellet for transmission-mode FT-IR measurements (<10 µm). The polymerization time is dependent on the oil (paint) thickness, and the time correlation among FT-IR and Raman-Brillouin data acquired in different samples (with an overall thickness of <10 µm) is assured by the comparison of the IR and Raman bands of the $(=C-H)_{cis}$ stretching mode marker of the isomerization proceeding (fig. S1, arrows).

Real microsample

A 1.6 mm by 1 mm (ca.) microfragment from the painting *Alchemy* (1947) was provided by the Peggy Guggenheim Collection (Venezia, Italy). The microfragment comes from a cold, opaque, paste-like white paint often applied by Pollock in the painting as final marks direct from the tube or as thin lines. Previous compositional investigations (*43*) indicated the presence of an oil paint mixture with a constant ratio of titanium and zinc white, probably from a ready-made formulation.

Combined micro–Brillouin-Raman

The combined Brillouin and Raman microspectroscopic setup consists of a 532-nm single-mode solid-state laser and a polarizing beamsplitter, which reflects the laser light into a 20× (numerical aperture, 0.42) microscope objective lens. The backscattered light is split in frequency and direction by an edge filter, so that the Stokes component (>30 cm^{-1}) is sent to a Horiba iHR320 Triax Raman monochromator, and the quasi-elastic and anti-Stokes components (<30 cm^{-1}) are sent to a high-contrast multipass tandem Fabry-Perot interferometer (TFP-2 HC, JRS Scientific Instruments) for simultaneous Raman

and Brillouin analysis. The sample is mounted on an *xyz* translation stage for single-point and mapping experiments. Each Brillouin-Raman spectrum was collected for about 1 × 60 s, using 600 lines/mm of grating and a 100-μm slit aperture in the range of 200 to 3000 cm^{-1}. Laser power on the sample was set to <10 mW. Any possible photodegradation was monitored by both visual checking through the microscope and in real-time monitoring of the Raman and Brillouin spectral features.

FT-IR spectroscopy

FT-IR spectroscopy was performed over the range of 4000 to 400 cm^{-1} by the Bruker Optics ALPHA-R spectrophotometer equipped with a SiC Globar IR radiation source, a Michelson interferometer RockSolid design), and a room-temperature DLaTGS detector. Transmission-mode spectra were recorded at a spectral resolution of 2 cm^{-1} and 100 acquisitions. FT-IR spectra acquired in transmission mode are plotted in absorbance after baseline subtraction and normalization to the C═O stretching mode at about 1740 cm^{-1}.

SUPPLEMENTARY MATERIALS

Supplementary material for this article is available at https://science.org/doi/10.1126/sciadv.abo4221

REFERENCES AND NOTES

1. L. de Viguerie, L. de Viguerie, G. Ducouret, F. Lequeux, T. Moutard-Martin, P. Walter, Historical evolution of oil painting media: A rheological study. *C. R. Phys.* **10**, 612–621 (2009).
2. M. Lazzari, O. Chiantore, Drying and oxidative degradation of linseed oil. *Polym. Degrad. Stab.* **65**, 303–313 (1999).
3. S. Pizzimenti, L. Bernazzani, M. R. Tinè, V. Treil, C. Duce, I. Bonaduce, Oxidation and cross-linking in the curing of air-drying artists' oil paints. *ACS Appl. Polym. Mater.* **3**, 1912–1922 (2021).
4. R. S. Morrell, H. R. Wood, *The Chemistry of Drying Oils* (E. Benn Ltd., ed. 1, 1925).
5. H. Wexler, Polymerization of drying oils. *Chem. Rev.* **64**, 591–611 (1964).
6. J. Honzíček, Curing of air-drying paints: A critical review. *Ind. Eng. Chem. Res.* **58**, 12485–12505 (2019).
7. I. Bonaduce, C. Duce, A. Lluveras-Tenorio, J. Lee, B. Ormsby, A. Burnstock, K. J. van den Berg, Conservation issues of modern oil paintings: A molecular model on paint curing. *Acc. Chem. Res.* **52**, 3397–3406 (2019).
8. J. van der Weerd, A. van Loon, J. J. Boon, FTIR studies of the effects of pigments on the aging of oil. *Stud. Conserv.* **50**, 3–22 (2005).
9. S. Keck, Mechanical alteration of the paint film. *Stud. Conserv.* **14**, 9–30 (1969).
10. T. J. S. Learner, P. Smithen, J. W. Krueger, M. R. Schilling, *Modern Paints Uncovered: Proceedings from the Modern Paints Uncovered Symposium* (Getty Publications, 2007).
11. L. Fuster-López, F. C. Izzo, M. Piovesan, D. J. Yusá-Marco, L. Sperni, E. Zendri, Study of the chemical composition and the mechanical behaviour of 20th century commercial artists' oil paints containing manganese-based pigments. *Microchem. J.* **124**, 962–973 (2016).
12. F. Scarponi, S. Mattana, S. Corezzi, S. Caponi, L. Comez, P. Sassi, A. Morresi, M. Paolantoni, L. Urbanelli, C. Emiliani, L. Roscini, L. Corte, G. Cardinali, F. Palombo, J. R. Sandercock, D. Fioretto, High-performance versatile setup for simultaneous Brillouin-Raman microspectroscopy. *Phys. Rev. X.* **7**, 031015 (2017).
13. L. Comez, D. Fioretto, F. Scarponi, G. Monaco, Density fluctuations in the intermediate glass-former glycerol: A brillouin light scattering study. *J. Chem. Phys.* **119**, 6032–6043 (2003).
14. L. Comez, C. Masciovecchio, G. Monaco, D. Fioretto, Progress in liquid and glass physics by brillouin scattering spectroscopy. *Solid State Phys.* **63**, 1–77 (2012).
15. C. E. Bottani, D. Fioretto, Brillouin scattering of phonons in complex materials. *Adv. Phys. X* **3**, 1467281 (2018).
16. F. Palombo, D. Fioretto, Brillouin light scattering: Applications in biomedical sciences. *Chem. Rev.* **119**, 7833–7847 (2019).
17. K. P. Menard, N. R. Menard, Ed., *Dynamic Mechanical Analysis* (CRC Press, 2020).
18. G. de Polo, M. Walton, K. Keune, K. R. Shull, After the paint has dried: A review of testing techniques for studying the mechanical properties of artists' paint. *Herit. Sci.* **9**, 68 (2021).
19. M. Bailey, M. Alunni-Cardinali, N. Correa, S. Caponi, T. Holsgrove, H. Barr, N. Stone, C. P. Winlove, D. Fioretto, F. Palombo, Viscoelastic properties of biopolymer hydrogels determined by Brillouin spectroscopy: A probe of tissue micromechanics. *Sci. Adv.* **6**, eabc1937 (2020).
20. S. Caponi, A. Passeri, G. Capponi, D. Fioretto, M. Vassalli, M. Mattarelli, Non-contact elastography methods in mechanobiology: A point of view. *Eur. Biophys. J.* **51**, 99–104 (2022).
21. M. A. Cardinali, D. Dallari, M. Govoni, C. Stagni, F. Marmi, M. Tschon, S. Brogini, D. Fioretto, A. Morresi, Brillouin micro-spectroscopy of subchondral, trabecular bone and articular cartilage of the human femoral head. *Biomed. Opt. Express* **10**, 2606–2611 (2019).
22. N. Correa, M. Alunni Cardinali, M. Bailey, D. Fioretto, P. D. A. Pudney, F. Palombo, Brillouin microscopy for the evaluation of hair micromechanics and effect of bleaching. *J. Biophotonics* **14**, e202000483 (2021).
23. D. Bersani, C. Conti, P. Matousek, F. Pozzi, P. Vandenabeele, Methodological evolutions of Raman spectroscopy in art and archaeology. *Anal. Methods* **8**, 8395–8409 (2016).
24. M. C. Caggiani, P. Colomban, Raman microspectroscopy for Cultural Heritage studies, in *Chemical Analysis in Cultural Heritage*, L. Sabbatini, I. D. van der Werf, Eds (De Gruyter, 2020), pp. 151–180.
25. S. Mattana, S. Caponi, F. Tamagnini, D. Fioretto, F. Palombo, Viscoelasticity of amyloid plaques in transgenic mouse brain studied by Brillouin microspectroscopy and correlative Raman analysis. *J. Innov. Opt. Health Sci.* **10**, 1742001 (2017).
26. R. Mercatelli, S. Mattana, L. Capozzoli, F. Ratto, F. Rossi, R. Pini, D. Fioretto, F. S. Pavone, S. Caponi, R. Cicchi, Morpho-mechanics of human collagen superstructures revealed by all-optical correlative micro-spectroscopies. *Commun. Biol.* **2**, 117 (2019).
27. M. A. Cardinali, M. Govoni, D. Dallari, S. Caponi, D. Fioretto, A. Morresi, Mechano-chemistry of human femoral diaphysis revealed by correlative Brillouin-Raman microspectroscopy. *Sci. Rep.* **10**, 17341 (2020).
28. M. Alunni Cardinali, A. Morresi, D. Fioretto, L. Vivarelli, D. Dallari, M. Govoni, Brillouin and Raman micro-spectroscopy: A tool for micro-mechanical and structural characterization of cortical and trabecular bone tissues. *Materials* **14**, 6869 (2021).
29. S. Caponi, S. Mattana, M. Mattarelli, M. Alunni Cardinali, L. Urbanelli, K. Sagini, C. Emiliani, D. Fioretto, Correlative Brillouin and Raman spectroscopy data acquired on single cells. *Data Brief* **29**, 105223 (2020).
30. S. Mattana, M. Alunni Cardinali, S. Caponi, P. D. Casagrande, L. Corte, L. Roscini, G. Cardinali, D. Fioretto, High-contrast Brillouin and Raman micro-spectroscopy for simultaneous mechanical and chemical investigation of microbial biofilms. *Biophys. Chem.* **229**, 123–129 (2017).
31. K. L. Ngai, R. Casalini, S. Capaccioli, M. Paluch, C. M. Roland, Dispersion of the structural relaxation and the vitrification of liquids, in *Fractals, Diffusion, and Relaxation in Disordered Complex Systems: Advances in Chemical Physics Part B* (JWS, 2006), pp. 497–593.
32. Y. Orlova, R. E. Harmon, L. J. Broadbelt, P. D. Iedema, Review of the kinetics and simulations of linseed oil autoxidation. *Prog. Org. Coat.* **151**, 106041 (2021).
33. B. Muik, B. Lendl, A. Molina-Díaz, M. J. Ayora-Cañada, Direct monitoring of lipid oxidation in edible oils by Fourier transform Raman spectroscopy. *Chem. Phys. Lipids* **134**, 173–182 (2005).
34. H. Sadeghi-Jorabchi, R. H. Wilson, P. S. Belton, J. D. Edwards-Webb, D. T. Coxon, Quantitative analysis of oils and fats by Fourier transform Raman spectroscopy. *Spectrochim. Acta Part A* **47**, 1449–1458 (1991).
35. V. Baeten, P. Hourant, M. T. Morales, R. Aparicio, Oil and fat classification by FT-raman spectroscopy. *J. Agric. Food Chem.* **46**, 2638–2646 (1998).
36. Z. O. Oyman, W. Ming, R. van der Linde, Oxidation of drying oils containing non-conjugated and conjugated double bonds catalyzed by a cobalt catalyst. *Prog. Org. Coat.* **54**, 198–204 (2005).
37. H. Kuhn, Zinc white, in *Artists' Pigments: A Handbook of Their History and Characteristics*, R. L. Feller, A. Roy, Eds. (Cambridge Univ. Press, 1986), pp. 169–186.
38. C. S. Tumosa, M. F. Mecklenburg, The influence of lead ions on the drying of oils. *Stud. Conserv.* **50**, 39–47 (2005).
39. L. F. Sturdy, M. S. Wright, A. Yee, F. Casadio, K. T. Faber, K. R. Shull, Effects of zinc oxide filler on the curing and mechanical response of alkyd coatings. *Polymer* **191**, 122222 (2020).
40. F. Gabrieli, F. Rosi, A. Vichi, L. Cartechini, L. P. Buemi, S. G. Kazarian, C. Miliani, Revealing the nature and distribution of metal carboxylates in Jackson Pollock's alchemy (1947) by micro-attenuated total reflection FT-IR spectroscopic imaging. *Anal. Chem.* **89**, 1283–1289 (2017).
41. C. Clementi, F. Rosi, A. Romani, R. Vivani, B. G. Brunetti, C. Miliani, Photoluminescence properties of zinc oxide in paints: A study of the effect of self-absorption and passivation. *Appl. Spectrosc.* **10**, 1233–1241 (2012).
42. J. J. Hermans, K. Keune, A. van Loon, R. W. Corkery, P. D. Iedema, Ionomer-like structure in mature oil paint binding media. *RSC Adv.* **6**, 93363–93369 (2016).
43. F. Rosi, C. Grazia, R. Fontana, F. Gabrieli, L. Pensabene Buemi, E. Pampaloni, A. Romani, C. Stringari, C. Miliani, Disclosing Jackson Pollock's palette in Alchemy (1947) by non-invasive spectroscopies. *Herit. Sci.* **4**, 18 (2016).
44. R. J. H. Clark, Q. Wang, A. Correi, Can the Raman spectrum of anatase in artwork and archaeology be used for dating purposes? Identification by Raman microscopy of anatase in decorative coatings on Neolithic (Yangshao) pottery from Henan, China. *J. Archaeol. Sci.* **34**, 1787–1793 (2007).

45. R. J. Jiménez Riobóo, C. Serrano-Selva, M. Fernández-García, M. L. Cerrada, A. Kubacka, M. Fernández-García, A. de Andrés, Acoustic and optical phonons in EVOH–TiO2 nanocomposite films: Effect of aggregation. *JOL* **128**, 851–854 (2008).
46. F. Modugno, F. Di Gianvincenzo, I. Degano, I. D. van der Werf, I. Bonaduce, K. J. van den Berg, On the influence of relative humidity on the oxidation and hydrolysis of fresh and aged oil paints. *Sci. Rep.* **9**, 5533 (2019).
47. L. Fuster-López, F. C. Izzo, V. Damato, D. J. Yusà-Marco, E. Zendri, An insight into the mechanical properties of selected commercial oil and alkyd paint films containing cobalt blue. *J. Cult. Herit.* **35**, 225–234 (2019).
48. A. Artesani, Zinc oxide instability in drying oil paint. *Mater. Chem. Phys.* **255**, 123640 (2020).
49. L. Baij, J. J. Hermans, K. Keune, P. Iedema, Time-dependent ATR-FTIR spectroscopic studies on fatty acid diffusion and the formation of metal soaps in oil paint model systems. *Angew. Chem. Int. Ed. Engl.* **57**, 7351–7354 (2018).
50. L. Baij, J. Hermans, B. Ormsby, P. Noble, P. Iedema, K. Keune, A review of solvent action on oil paint. *Herit. Sci.* **8**, 43 (2020).
51. M. F. Mecklenburg, C. S. Tumosa, Traditional oil paints: The effects of long-term chemical and mechanical properties on restoration efforts. *MRS Bull.* **26**, 51–54 (2001).
52. S. Corezzi, L. Comez, M. Zanatta, A simple analysis of Brillouin spectra from opaque liquids and its application to aqueous suspensions of poly-N-isopropylacrylamide microgel particles. *J. Mol. Liq.* **266**, 460–466 (2018).
53. R. J. Gettens, G. L. Stout, *Painting Materials: A Short Encyclopaedia* (Courier Corporation, Dover Publications, 1966).
54. Ö. K. Güler, F. S. Güner, A. T. Erciyes, Some empirical equations for oxypolymerization of linseed oil. *Prog. Org. Coat.* **51**, 365–371 (2004).
55. A. P. Laurie, The refractive index of a solid film of linseed oil: Rise in refractive index with age. *Proc. R. Soc. Lond. A*, **159**, 123–133 (1937).
56. D. Fioretto, S. Corezzi, S. Caponi, F. Scarponi, G. Monaco, A. Fontana, L. Palmieri, Cauchy relation in relaxing liquids. *J. Chem. Phys.* **128**, 214502 (2008).
57. G. Monaco, D. Fioretto, L. Comez, G. Ruocco, Glass transition and density fluctuations in the fragile glass former orthoterphenyl. *Phys. Rev. E Stat. Nonlin Soft Matter Phys.* **63**, 061502 (2001).
58. R. S. Berns, E. R. de la Rie, The effect of the refractive index of a varnish on the appearance of oil paintings. *Stud. Conserv.* **48**, 251–262 (2003).
59. R. L. Feller, Factors affecting the appearance of picture varnish. *Science* **125**, 1143–1144 (1957).
60. P. Vandenabeele, B. Wehling, L. Moens, H. Edwards, M. De Reu, G. Van Hooydonk, Analysis with micro-Raman spectroscopy of natural organic binding media and varnishes used in art. *Anal. Chim. Acta* **407**, 261–274 (2000).
61. M. Gomez, D. Reggio, M. Lazzari, Linseed oil as a model system for surface enhanced Raman spectroscopy detection of degradation products in artworks. *J. Raman Spectrosc.* **50**, 242–249 (2019).

Acknowledgments: We acknowledge the Peggy Guggenheim Collection (PGC) for providing the microfragment from the *Alchemy* painting. **Funding:** This work was funded by IPERION HS, H2020-INFRAIA-2019-1, under GA no. 871034 (to F.R., L. Ca., and C.M.).
Author contributions: Conceptualization: F.R., L.Co., M.P., C.M., and L.P.B. Methodology: F.R., L.Co., and M.A.C. Investigation: M.A.C. and L.Co. Visualization: F.R., L.Co., and M.A.C. Supervision: F.R. and L.Co. Writing—original draft: F.R., L.Co, M.A.C., and L.Ca. Writing—review and editing: F.R., L.Co., M.A.C., L.Ca., M.P., D.F., and L.P.B. **Competing interests:** The authors declare that they have no competing interests. **Data and materials availability:** All data needed to evaluate the conclusions in the paper are present in the paper and/or the Supplementary Materials.

Submitted 4 February 2022
Accepted 12 May 2022
Published 29 June 2022
10.1126/sciadv.abo4221